DEVELOPMENT, PRODUCTION AND POST-PROCESSING OF A TOPOLOGY OPTIMIZED AIRCRAFT BRACKET

Helge Klippstein[1], Anne Duchting[2], Thomas Reiher[2], Florian Hengsbach[1], Dennis Menge[1],
Hans-Joachim Schmid[1]

[1] Direct Manufacturing Research Center and Particle Technology Group,
Paderborn University, Germany
[2] simufact engineering GmbH, Paderborn, Germany

Contact: Helge.Klippstein@dmrc.de

Abstract

Structural parts for aviation have very high demands on the development and production process. Therefore, the entire process must be considered in order to produce high-quality AM metal parts. In this case study, a conventional part was selected to be optimized for AM. The process presented includes component selection, design improvement with a novel approach for topology optimization based on the AMendate algorithm as basis of MSC Apex Generative Design, component production on a SLM 250 HL and post-processing including heat treatment and surface smoothing. With the topology optimization a weight reduction of ~60 % could be realized, whereby the stress distribution is more homogeneous. Furthermore, the challenges of support optimization and post-processing have to be addressed, in order to produce competitive parts.

Introduction

The additive manufacturing technology is characterized typically by the multi-layer composition of the components. Altogether, the research and application area for additive manufacturing is a growing market with often so-called "endless potentials". This can be deduced from the number of publications and patents which have increased significantly since 2014 [1]. At the same time, the number of AM technologies and companies continues to grow.

Additive manufacturing is particularly attractive, if the part is highly complex and/or the number of parts per series is relatively small [2]. Applying Design for Function instead of the traditional Design for Manufacturing approach and including part consolidation and integration, increases the complexity of parts and assemblies. At the same time, weight, maintenance and waste reduction can be achieved by using generative manufacturing techniques. In addition, the combination of CAD/CAM and AM will shorten development times [3]. In aviation, this as well as the weight saving potential or the reduction of tooling and warehouse costs should be taken into considerations by calculating a business case for AM parts [4, 5]. The production of conventional part designs with AM technology contradicts the overriding objectives of AM and aircraft design. Only by leveraging the design freedom of AM technology this process will be truly competitive, raising both performance potentials and cost savings [6]. This is as well reflected in the new approach by *Airbus*, targeting clean sheet design solutions for the AM implementation [1].

Due to the high quality requirements and regulations in the aviation sector, the implementation of AM technology is closely associated with very expensive material and process qualifications. The

ASTM F42 and ISO TC 261 committees, namely the most important qualification committees, work on universal guidelines for the AM qualification process [7]. However, up to now there are only a few materials and processes qualified.

Today, Boeing and Airbus have already implemented thousands of generative manufacturing parts for civil and military systems. Since ULTEM 9085, PEEK and PEKK are one of the first AM materials suitable for aviation, most of these parts are manufactured using FDM technology. However, the trend towards more metal parts is obvious as several metal AM parts today are qualified and flying.

In general there are three approaches for qualification:
    a) Statistical qualification
    b) Equivalence-based qualification
    c) Model based qualification.

Whereby, version a) leads to costly empirical tests, the equivalence-based qualification is linked to the statistical qualification and reduces therefore the required amount of tests, e.g. for a new material on the same machine. The model based qualification is supported by an in detail understanding of the process and related simulations [8]. For example, to certify the GE9X T25 sensor and LEAP fuel nozzle from GE, massive pre-testing was done to guarantee repeatable results. Hereby, the overall process is qualified for this part [1, 9]. However, with progress done in process qualification, the door can be opened for equivalence-based material or part qualification. Furthermore, with improved process simulations, even validated model-based qualification with high accuracy can be realistic in the future. Additionally, the concept of "qualify as you go" might be applied. Hereby, multiple pre-, in- and post-process measurements shall demonstrate that a part will perform as specified [8].

As soon as more AM companies, processes, parts and materials are qualified, the spare part market might become more important. In future, the spare part could be manufactured on site and therefore reduce warehouse and shipping costs [3, 5, 10, 11]. To reach this bright future scenario, it is important to increase the number of flying AM parts further more.

When using AM on existing parts, the biggest challenge is to identify promising candidates. The search for these parts is much more difficult than setting up a new part from scratch, as the business case must cover all change costs, including changes to manufacturing drawings, component lists, possible fastener adjustments, quality checks, maintenance and repair guidelines, etc. However, within this study an existing aircraft bracket was identified and redesigned for additive manufacturing based on the Laser Beam Melting (LBM) process.

Methodology and Original Bracket

The bracket identified here is installed less than 100 times a year. It is an assembly of two aluminium brackets milled from solid raw material with a buy-to-fly ratio of approximately 6.25. The boundary box of this part is around 100 x 110 x 120 mm. Based on the part size, cost above average for conventional brackets and small number of parts per year this assembly was chosen for redesign and replacement by an AM part. Related to assembly situation, only the load direction for the attacking forces is known but not the size of those forces. Starting from the load direction, the load capacities and limiting loads are determined by reengineering (Figure 1). The two brackets are preassembled by rivets and fastened to the structure. A FEA is executed for each load case with an arbitrary load of 1 N. Based on the stress and the deformation in load direction, the ultimate-, limit load and bracket stiffness in load direction are determined (1-3).

$$ultimate\ load = \frac{normalized\ load\ (1N)}{maximal\ Von\ Mises\ stress} * material\ yield\ strength \quad (1)$$

$$limit\ load = \frac{ultimate\ load}{safty\ factor\ (1.5)} \quad (2)$$

$$stiffness\ in\ load\ direction = \frac{normalized\ load\ (1N)}{displacement\ in\ load\ direction} \quad (3)$$
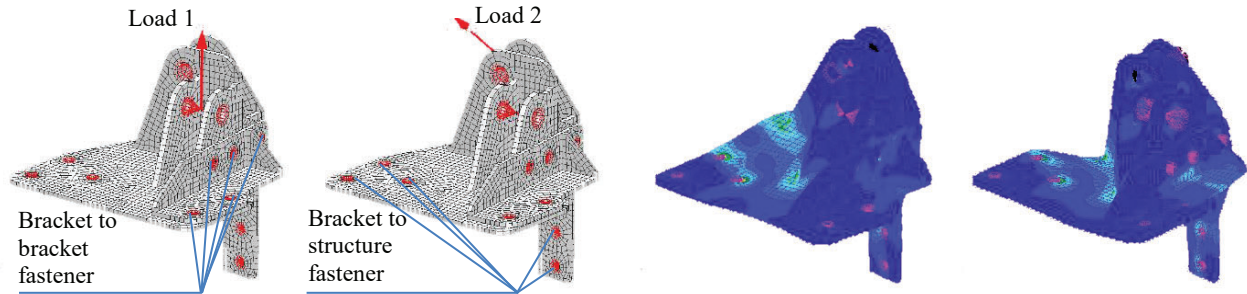

Figure 1 Original aircraft bracket with two load cases and the related Von Mises stress distribution per loadcase

The new part shall be designed for the LBM technology with AlSi10Mg powder. Several aviation and AM companies do work hard for the qualification of this material [12]. The part manufacturing is done with an *SLM-250HL* from *SLM Solutions*. First a topology optimization (TO) is carried out. This design is further adapted to the LBM-related design guidelines and then manufactured. The parts are reworked and all functional areas are milled as part of the finishing process. Finally, a static test validation of the fixture is carried out on a uniaxial tensile testing machine.

AlSi10Mg - Material Properties

For the topology optimization and the FEA validation a close look has to be given to the fatigue behavior of AlSi10Mg LBM parts, as still most parts fail due to dynamic loads [13]. Based on the properties of the conventional bracket, dynamic load cases have been calculated and applied to the TO design. A fatigue strength at the ratio R = σ_{min}/ σ_{max} = 0.1 is required for the new design. LBM aluminium parts are known to have a higher yield and ultimate strength, compared to conventional aluminium parts. The microstructure of LBM "as build" parts is very fine due to the extremely high cooling rates [14, 15]. In contrast, the elongation at break and fatigue strength is in the as build condition mostly lower than the conventionally manufactured counterpart.

Several approaches have been made to improve the fatigue resistance of LBM parts. Most promising are surface smoothing and heat treatment. As well, remaining powder moisture has an influence on the porosity and the correlated part density which in turn influences the life time [16]. Obviously, there are multiple additional influencing factors for the part quality. The fatigue information gathered in Table 1 are based on literature values with different treatment methods. There are samples with different scanning parameters, layer thicknesses, build platform temperatures, machines or orientations included to the table. In every case only the weakest sample set is displayed per treatment method.

Source	Load Ratio	Machine	Cycles	Weakest σ_{max}	Post treatment
[15]	R = 0.1	Trumpf TrumaForm LF130	$\sim$5.5x10^6	$\sim$90 MPa	machined
			5x10^7	$\sim$100 MPa	machined
			5x10^7	$\sim$140 MPa	T6* heat treated and machined
[17]	R = 0.1	Renishaw AM250 SLM	7.6x10^6	63 MPa	as build
			3x10^7	94 MPa	T6* heat treated
			3x10^7	126 MPa	T6* heat treated and machined
[18]	R = -1	EOS M400	2x10^7	140 MPa	machined
[19]	R = -1 rotating beam mode	unknown	1x10^7	$\sim$50 MPa	as build
			1x10^7	$\sim$90 MPa	polished
[20]	R = -1	EOSINT M-280	3x 10^7	50 MPa	machined and polished + HIP*** 500°C
			1x 10^7	$\sim$75 MPa	stress relieved (300°C / 2h) machined and polished
			1x 10^7	$\sim$125 MPa	machined or polished
[21]	R = -1 rotating beam mode	EOSINT M-270	5x10^6	97±7 MPa	as build
[22]**	R=0.1	EOSINT M-280	1x10^5	178 MPa**	stress relieved (300°C / 2h) machined
			3 x10^4	222 MPa**	stress relieved (300°C / 2h) machined

With the information of Table 1 the maximal stress for the topology optimization and FEA validation can be deduced. *EOS GmbH* and *SLM Solutions AG* suggest a heat treatment for two hours at 300°C, as the typical microstructure of LBM parts is already close to the one obtained after T6 heat treatment [21, 23]. In contrast, Uzan et al. [20] have experienced a life time reduction by the stress relief procedure whereby large pores within the fracture surface were observed. However, the life cycle points checked by Tang et al. do indicate a much better performance of parts annealed by stress relief [22]. The large variety of obtained mechanical properties substantiate that the effects of e.g. machine- and exposure setting, powder properties and testing procedure have significant influences on the results.

Most of the data presented in the table are related to the stress ratio of R = -1, whereby the bracket under consideration here is loaded by the ratio R = 0.1, which in general allows higher maximal loads than at R = -1 ratio. Within the post processes a stress relief heat treatment is planned. Even surface smoothing operations will be investigated. Thus, for simulation of the bracket a fatigue

strength of 80 MPa has been assumed, which appears to be well in the range of the literature values and covers uncertainties of process parameters with a factor of 1.17 for just heat treated [17] and 1.25 for machined samples from [15]. The used material properties are related to the powder, machine and exposure settings. The most important exposure parameters are presented in Table 2 whereby the material properties are cumulated based on literature values [15, 17–22].

Table 2 Material Properties and exposure settings

Properties after heat treatment (as provided by powder manufacturer)			Contour	Volume
E-Modul	59 GPa	Scan speed	500 mm/s	930 mm/s
Yield strength	205 MPa	Laser power	350 W	350 W
Ultimate strength	250 MPa	Hatching spacing	170 μm	170 μm
Elongation at break	~9 %	Laser focus	80 μm	80 μm
Fatigue strength	~80 MPa			
		Platform heating	200°C	
		Layer Resolution	50 μm	

Topology Optimization

Starting point of the optimization is the conventional bracket assembly as shown in Figure 2. Combining the dark green and dark red bracket much more three-dimensional optimization potential is generated, as well as the benefits of part reduction. The bracket has five bolt connections to the airframe, as marked in yellow in Figure 2.
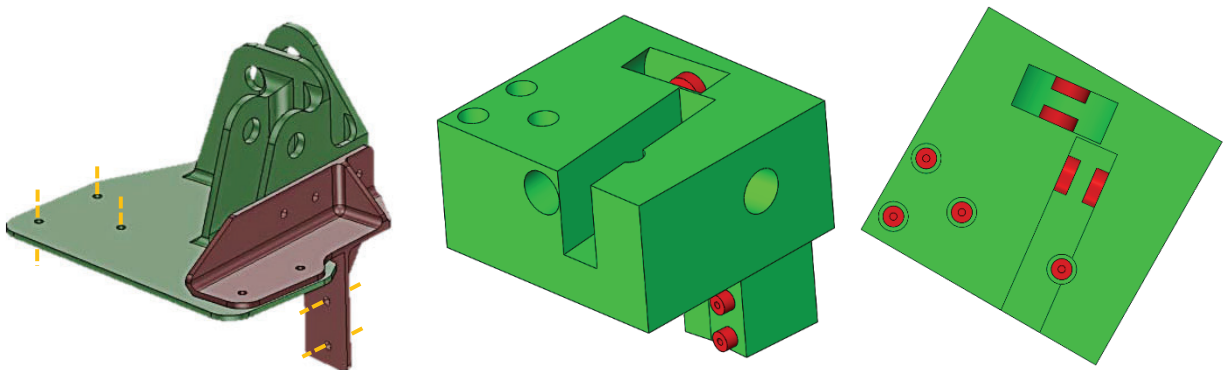

Figure 2: Left graphic: Conventional bracket composition with main bracket (dark green) and additional bracket (dark red). On the right: Design space (green) and non-design space (red) for topology optimization

For the design optimization there is a general principle used that is called "topology optimization" (TO). Topology optimization is an automated extension for FEM based structural analysis. With this iterative procedure a technical component can be optimized by changing its geometry regarding different characteristic values. Most of the commercially available TO-software offers optimization goals such as mass reduction at a given stiffness or a stiffness maximization at a permitted mass. At the same time, the permitted strength must not be exceeded to ensure the structural integrity. For most TO-processes, an additional FE-analysis is needed to validate the occurring stresses of the final design.

The process of topology optimization starts with a model setup, according to the classical FE analysis including loads and external constraints on all interface areas. To run a proper topology overall geometry is divided in a "design space" where material is allowed but not mandatory, and the "non-design space", where material is mandatory as for interfaces such as bolts or bearing seats. To enable the optimization algorithm to generate best designs, it needs to have the most possible design freedom, what is achieved with a design space that is as large as possible. It can be a simple but massive geometry or an arbitrary complex one as in complex assemblies, which defines the maximum allowed material for the component. By solving the FE calculation, stress and strain can be determined for each of the elements located in this design space. The optimization algorithm now decides which of the elements can be removed without exceeding given restrictions such as displacement or stress maxima. Subsequently, a new analysis is performed with this reduced amount of material, the element stresses are interpreted, and further material is removed or reattached. Performing this iterative procedure, the optimization algorithm approaches an optimal component shape step by step.

For this part the design space is created considering the adjacent components and is designed as generously as possible. It should also be noted that the nondesign spaces must be accessible for assembling and therefore material must be left out. The result can be seen in Figure 2 with the design space marked green and non-design space marked red.

The software solution "*AMendate*" was used for the optimization of the bracket. *AMendate* is a topology optimization software that has been developed by a young start-up of former DMRC-employees from Paderborn University and is now part of the commercially available software solution "MSC Apex Generative Design 2019". The main difference of this "generative design" tool towards most known topology optimization tools is the automated interpretation and definition of a final geometry during the optimization. This enables the use of a clearly defined stress goal instead of the beforehand mentioned ones: mass reduction or stiffness. As for other optimization tools, during the optimization the material is reduced based on the FE results. Though, in each iteration a specific design with a geometrically and mechanically useful surface is generated. Thus, the user does not need to interpret the results and do manual redesign in a CAD-system. Each design is analyzed by the algorithm regarding the occurring stresses in detail. This is possible due to a completely new approach that is not based on the popular SIMP-algorithm (solid isostatic material with penalization) which gives a varying density to each element, but on a so called hard-kill algorithm. In these algorithms the elements considered to be unimportant for the structure with low stress or strain are fully deleted and not considered in further iterations. This hard decision enables a generation of a high quality part surface and thus determination of a clearly distinct structure [28].

The software allows to influence the generated design in terms of complexity like a more "filigree" design with many small struts and thin shells or with a more "massive" design with less but thicker elements. Three versions have been calculated as shown in Figure 3. Hereby, the violet (rough) and orange (normal) bracket do variate in weight about 0.1 g, whereby the blue (filigree) bracket weights 2.7 g more than the orange one. All brackets have similar maximum stress levels and do not violate the 80 MPa limit. The stiffness of the orange one is the highest. An additional criteria for the design selection is the amount of attachment points. The violet (rough) design has only three bolt connections to the airframe. For safety considerations, it can be expected, that additional fastening connections and therefore struts will lead to a more good-natured failure pattern. Hence, the normal setting is used for further development, it is based on stress and stiffness very good, has multiple fastening points and as well the structure is not too filigree.

Compared to bulky parts, thin structures do show much weaker mechanical properties due to an increased ratio of contour to volume exposure and therefore increased porosity [14, 24]. These imperfections should be taken into account when evaluating the results of topology optimization. In particular, the very filigree struts cannot withstand the calculated loads of the FEA. Therefore, an offset is given to the overall design and all functional areas are thickened to allow subtractive post-processing. The areas subject to higher loads are additionally reinforced. The manual rework is done together with the support optimization of the bracket.

Figure 3: Three different TO results from left to right with more filigree structures. Based on the filigree settings three (rough result – left bracket) up to five (very filigree result – right bracket) attachment points are used. The final design with is developed further is the orange one with four attachment point.

Support Optimization

For the LBM manufacturing process a supporting structure is required. Based on the AM design guidelines, the build orientation should be specified at the beginning of the design process, since it has several influences on the component properties [25]. For topology optimization without a support optimization algorithm, however, the build orientation must be checked first. The software *Magics* from *Materialise* and *Meshmixer* from *Autodesk* are used to optimize the build orientation. Within this software, the STL file and orientation can be analyzed and optimized for various purposes. These algorithms are based on the triangle orientation of each surface element in the STL file. This allows a threshold overhang angle to be defined related to the process and the material. All triangles with an orientation smaller than this angle should be checked for support requirements. The objective of the optimization used here is to minimize the summed up projected area on the X-Y plan. For post-processing, the inner support structure, which grows from part to part, is particularly critical as it is difficult to remove and leaves double marks on the component surface, one on the underside and one on the top.

In the LBM process, the purpose of the support is not only to keep the material in place, it is also required for heat dissipation. With aluminium, the cone support in particular fulfils this purpose, as the contact surface of the line or block support with tooth is very small. Experience shows stable structures with good surface properties up to an overhang angle of 35°. In the literature even smaller angles can be built, but the surface roughness increases significantly [26]. Newer LBM machine generations do support special overhang parameter settings whereby the trend is even going to much smaller angles with different exposure strategies and laser controls, e.g. pulsed laser [27].

The purpose of the following procedure is to adapt the part design, in order to reduce the overall support area. Particularly, the struts supported internally should be removed. Small holes and voids are filled up. The part is sculpted to reduce overhangs to a limit of 35° which is shown in Figure 4. Within this procedure the orientation angle is checked again and fine part orientation adjustments based on the small modifications are done. The comparision of the original TO version and the support addapted one shows significantly smaller overhang areas and therefore less required support. Areas with two struts merging together, called bridging, do not need to be supported as the part itself supports the structure efficiently. Aliminium is not very sensitive for residual stress deformation during the build process, still additional cone supports has been added to the functional areas of the bracket to reduce deformation due to residual stress. Test build jobs with both designs have shown, that the postprocessing of the support adapted design is more than 10 times faster, as the standard TO design and takes around 2 minutes for the rough support removal and 15 minutes for mechanical smoothing of the attachment areas.
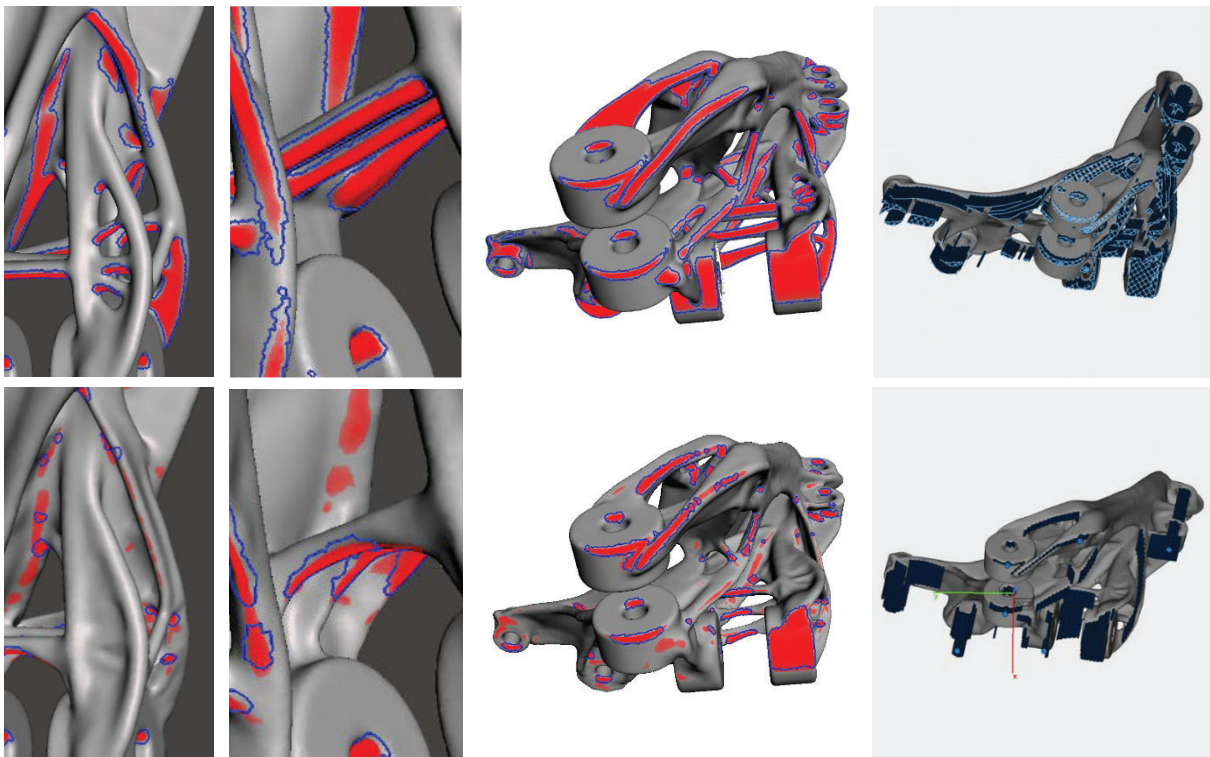

Figure 4 Optimized build orientation with reduced support area and less numbers of merging struts; Overhang angle of 35° marked in red. Top row displays the TO output brackets, bottom row shows the adapted design. Left: close ups of examples for the modifications: filled up voids and sculptured struts to avoid part to part support. Middle: Bottom View, support surfaces in red, right: bottom view of the applied support structure

Finite Element Analysis

Finally, the results of the topology optimization and the part adaptions for quickly removable support structure, need to be validated. Based on a finite element analysis, the part is tested for static and fatigue behavior. The software *Solidworks 2018* from *Dassault Systèmes* was used for the validation.
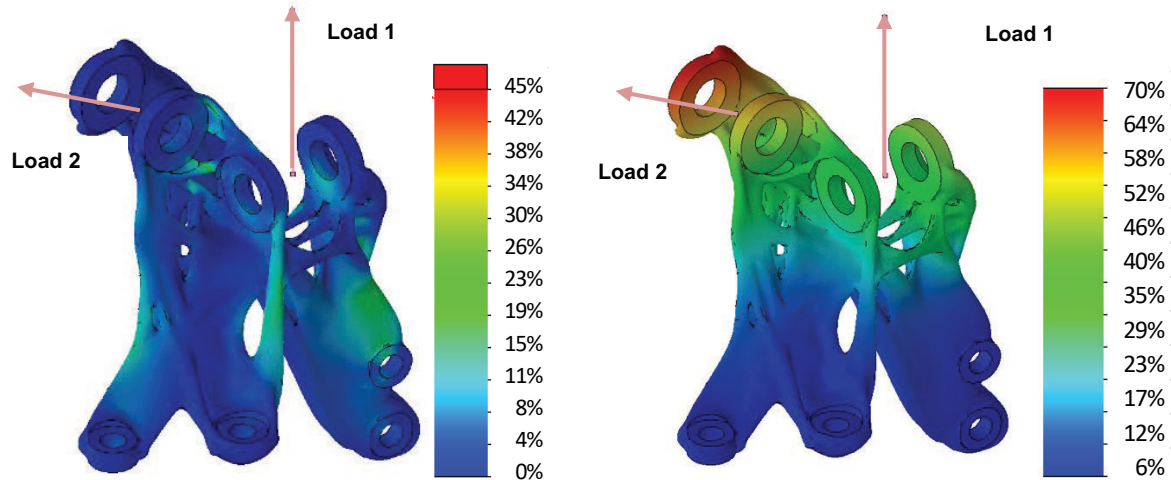
Figure 5 TO-Bracket validation, left Von Mises stress (normalized to maximal stress of the original bracket) right: deformation (normalized to maximal deformation of the original bracket)

By comparing the FEA results of the TO bracket to the FEA of the conventional bracket, it becomes clear, that the stiffness of the part has increased. The new design can hold three times higher loads of the first load case and 2.1 times higher loads in the second load direction. Therefore, load two is the limiting load, as the initiated stresses within the bracket are higher. Hence, load two is used as the validation load for the bracket tested on a uniaxial tensile test machine. Combining both loads, the maximal stress of the bracket reach 114 MPa for the ultimate load and thus 75 MPa for the limit load. Applying disturbance loads by vary the load direction of both loads about 10° shows a maximal stress increase of ~25% to 96 MPa. After further thickening of the highly loaded struts a rerunning of the analysis reveals that the disturbance load impact is reduced to 5% stress increase. The bracket is therefore designed close to the limit and will withstand the limiting fatigue stress level of 80MPa. However, in order to master the ultimate load in cyclic loading, the bracket should be finished furthermore. Another option would be to further inflate the highly loaded struts.

Manufacturing, Post Processing and Finishing

The brackets are manufactured on a *SLM 250-HL* from *SLM Solutions* which is running on build processor 2.2 and cannot apply overhang parameter settings. As the powder moisture does have a significant influence on the part quality, the powder was dried prior to the process. With dry powder the hydrogen porosity can be reduced significantly as well as a better part surface can be obtained due to the reduction of weld spatter [16]. 35 cycles of vacuum drying and argon rinsing can dry around 5 kg of aluminium powder within 35 minutes. The machine runs for 26 hours with a job height of 110 mm to manufacture eight parts on one build platform. These work cycle times can be reduced on modern multi-laser machines to improve the business case.

To reduce tension and potential deformation, as well as to obtain a higher ductility of the brackets, the build brackets mounted on the build platform are stress relief annealed.

After removing the support structure and smoothing the attachment marks manually, all functional surfaces, as displayed in Figure 6, are milled. All brackets are blasted with corund, followed by glass bleads.

Figure 6 Functional surface of the bracket in red and overview of the brackets during unpacking of the build job

Static Test Validation

For the static test of the bracket, it is loaded in the direction of load case two which indicates higher stresses within the bracket. The specimen is fixed on a massive steel block at the bottom of the tensile test machine. As displayed in Figure 7, the load is applied via attachment point B in an angle of 30°. The attachment point A for load one is bolted together as a part of the stresses applied by load two will be guided through this connection, which has a bolt connection even in the real assembly. All fixing points from the bracket to the rig as well as the load attachments are prepared with engineering fit H7.

Especially in the beginning of the load curve the gradient is not linear (Figure 7). It is expected, that not all struts are loaded equally, thus the final stiffness of the bracket is reached first at around 80% load. The required ultimate load of the conventional (original) bracket is withstood by the new design without fail. The component has passed the test for the calculated limit and ultimate load intact, as well. At 225% load the limits of the test set up are reached. Thus, the bracket could not be run in a destructive test.
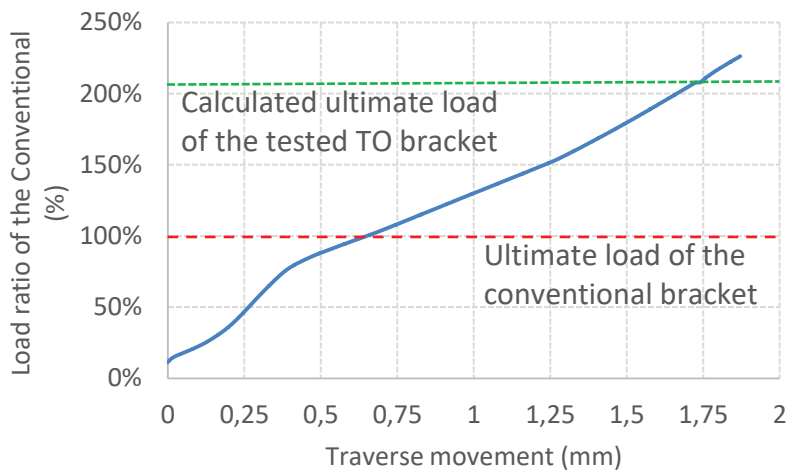

Figure 7 Static validation of the support optimized TO-bracket, Left: the bracket in assembled on the test rig for load 2 attacking in 30° on attachment point B. Load 1 attachment point (A) is bolted together to simulate the additional stiffening connection. Right: Topology optimized bracket test diagram. Test stop without failure at 225 % of the load related to the original (conventional) bracket.

In combination with the engineering fit connections and the assumption, that the test rig made of steel and fixed by steel 8.8 screws is much stiffer than the aluminium bracket, it can be expected that the traverse movement is equal to the elongation of the bracket in load direction. Here it is essential, that the elongation for the 100% load of 0.65 mm is much higher than calculated by the FEA. Whereby, with 59 GPa the used E-Modulus for the FEA material model is already conservative.

Additionally a fatigue test of the bracket design has been run at 20 Hz with a tension load ratio of R = 0.1 for load case two. Hereby the load pattern follows a sinus curve. The test was performed on a Zwick/Roell HC10 servohydraulic testing machines, whereby the bracket is bolted to the same test rig, as used for the static test. After ~4,670,000 cycle loads the test was stopped due to a violation of the lower stress limit. By restarting the test some massive stress limit violations led to a total fail of the part short after the restart of the machine. SEM images has been taken to analyze the failure pattern as presented in Figure 8. Here the crack initiation, propagation as well as resting lines and the final fracture zone can be seen. Very prominent are the amount of pores and unmolten particles, exemplary marked in violet at the bottom left image of Figure 8. It was found, that the used SLM machine had a defect laser, which could not deliver the set laser power. Hence the part validation has to be repeated. However, even with those drawbacks the bracket has withstood close to 4.7 million cycles as well as the static stress tests.
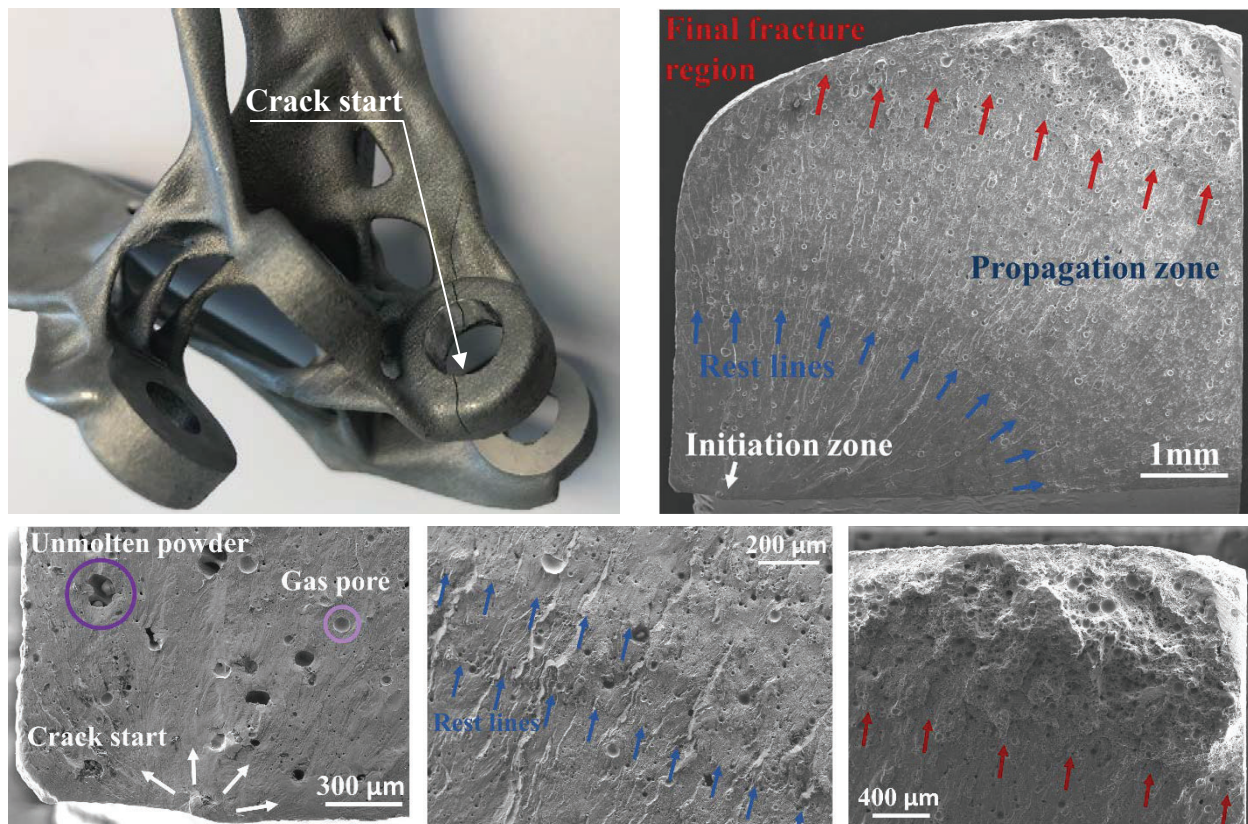

Figure 8 Bracket after dynamic tests. Top left: crack line through the bracket. Top right: SEM image of the fracture zone. Bottom left: crack initiation point. Bottom middle: rest lines and Bottom right: final fracture region

Conclusion and Outlook

It has been shown, that performance improvements can be achieved by topology optimization and additive manufacturing. The support optimization for the LBM process is hereby still in focus, which leads to manual design adaptations. However, the company *AMendate* is working on an optimization algorithm for their software, to generate support optimized TO results. This in turn will reduce the required design effort after the TO dramatically. Furthermore, the individualities of the LBM process need to be considered for every FEA analysis, as these structures often show imperfections, which are related to a complex process. Powder drying helps already to improve the process stability and part quality. Still differences between simulations and real build part tests can be seen, e.g. in the predicted fracture region. Hereby the impact of the lately detected laser defect could be a reason for this and at least for the high porosity within the parts. Hence, at least for machines without a melt pool monitoring system additional test samples are recommended for every build job with critical parts.

The work done for this bracket shows the potential of AM. As soon as the material is qualified for civil aviation applications, multiple brackets like this, could be replaced as weight savings of around 60% can be achieved additionally with improved performance. Statically test have shown, that the material model used for the FEA simulation seems to be conservative. The dynamic testing of the bracket is a very important step towards AM structural parts in aviation and need to be repeated for this bracket. Only if the high cycle fatigue demands are fulfilled, this part will fly.

Acknowledgement

References

References
[1] T. Wohlers, R. I. Campbell, and O. Diegel, *Wohlers report 2018: 3D printing and additive manufacturing state of the industry : annual worldwide progress report*. Fort Collins, Colo.: Wohlers Associates Inc, 2018.
[2] A. Gebhardt, *Generative Fertigungsverfahren: Rapid Prototyping - Rapid Tooling - Rapid Manufacturing,* 3rd ed. München: Hanser, 2007.
[3] R. Huang *et al.,* "Energy and emissions saving potential of additive manufacturing: The case of lightweight aircraft components," *Journal of Cleaner Production*, vol. 135, pp. 1559–1570, 2016.
[4] R. E. Laureijs *et al.,* "Metal Additive Manufacturing: Cost Competitive Beyond Low Volumes," *J. Manuf. Sci. Eng*, vol. 139, no. 8, p. 81010, 2017.
[5] G. Deppe, "Exploring the supply chain opportunities of Additive Manufacturing in aviation's spare part industry,"
[6] C. Lindemann, T. Reiher, U. Jahnke, and R. Koch, "Towards a sustainable and economic selection of part candidates for additive manufacturing," *Rapid Prototyping Journal*, vol. 21, no. 2, pp. 216–227, 2015.

[7] A. Uriondo, M. Esperon-Miguez, and S. Perinpanayagam, "The present and future of additive manufacturing in the aerospace sector: A review of important aspects," *Proceedings of the Institution of Mechanical Engineers, Part G: Journal of Aerospace Engineering*, vol. 229, no. 11, pp. 2132–2147, 2015.

[8] M. Shawn P., *Qualification for Additive Manufacturing Materials, Processes, and Parts.* [Online] Available: https://www.nist.gov/programs-projects/qualification-additive-manufacturing-materials-processes-and-parts. Accessed on: 06.2019.

[9] M. Seifi, A. Salem, J. Beuth, O. Harrysson, and J. J. Lewandowski, "Overview of Materials Qualification Needs for Metal Additive Manufacturing," *JOM*, vol. 68, no. 3, pp. 747–764, 2016.

[10] A. Ceruti, P. Marzocca, A. Liverani, and C. Bil, "Maintenance in Aeronautics in an Industry 4.0 Context: The Role of Augmented Reality and Additive Manufacturing," *Journal of Computational Design and Engineering*, 2019.

[11] J. C. Najmon, S. Raeisi, and A. Tovar, "Review of additive manufacturing technologies and applications in the aerospace industry," in *Additive manufacturing for the aerospace industry*, F. H. Froes, Ed., Amsterdam, Netherlands, Cambridge, MA, United States: Elsevier, 2019, pp. 7–31.

[12] B. Sagel, *NextGenAM – Pilotprojekt für automatisierten metallischen 3D-Druck ein voller Erfolg: Pressemitteilung.* [Online] Available: https://www.premium-aerotec.com/medien/pressemeldungen/nextgenam-pilotprojekt-fuer-automatisierten-metallischen-3d-druck-ein-voller-erfolg/.

[13] F. C. Campbell, *Fatigue and Fracture: Understanding the basics*, 2012.

[14] Z. Dong *et al.,* "Study of Size Effect on Microstructure and Mechanical Properties of AlSi10Mg Samples Made by Selective Laser Melting," (eng), *Materials (Basel, Switzerland)*, vol. 11, no. 12, 2018.

[15] E. Brandl, U. Heckenberger, V. Holzinger, and D. Buchbinder, "Additive manufactured AlSi10Mg samples using Selective Laser Melting (SLM): Microstructure, high cycle fatigue, and fracture behavior," *Materials & Design*, vol. 34, pp. 159–169, 2012.

[16] C. Weingarten *et al.,* "Formation and reduction of hydrogen porosity during selective laser melting of AlSi10Mg," *Journal of Materials Processing Technology*, vol. 221, pp. 112–120, 2015.

[17] N. T. Aboulkhair, I. Maskery, C. Tuck, I. Ashcroft, and N. M. Everitt, "Improving the fatigue behaviour of a selectively laser melted aluminium alloy: Influence of heat treatment and surface quality," *Materials & Design*, vol. 104, pp. 174–182, 2016.

[18] S. Romano *et al.,* "Fatigue properties of AlSi10Mg obtained by additive manufacturing: Defect-based modelling and prediction of fatigue strength," *Engineering Fracture Mechanics*, vol. 187, pp. 165–189, 2018.

[19] T. M. Mower and M. J. Long, "Mechanical behavior of additive manufactured, powder-bed laser-fused materials," *Materials Science and Engineering: A*, vol. 651, pp. 198–213, 2016.

[20] N. E. Uzan, R. Shneck, O. Yeheskel, and N. Frage, "Fatigue of AlSi10Mg specimens fabricated by additive manufacturing selective laser melting (AM-SLM)," *Materials Science and Engineering: A*, vol. 704, pp. 229–237, 2017.

[21] W. AD, "EOS Aluminium AlSi10Mg," https://lightway-3d.de/download/LIGHTWAY_EOS_Aluminium_AlSi10Mg_de_Datenblatt.pdf, 2014.

[22] M. Tang and P. C. Pistorius, "Oxides, porosity and fatigue performance of AlSi10Mg parts produced by selective laser melting," *International Journal of Fatigue*, vol. 94, pp. 192–201, 2017.

[23] SLM Solutions Group AG, "Al-Alloy AISi10Mg / EN AC-43000 / EN AC-AISi10Mg," https://www.slm-solutions.com/fileadmin/user_upload/MDS_Al-Alloy_AlSi10Mg_0219.pdf, 2012.

[24] Y. Amani, S. Dancette, P. Delroisse, A. Simar, and E. Maire, "Compression behavior of lattice structures produced by selective laser melting: X-ray tomography based experimental and finite element approaches," *Acta Materialia*, vol. 159, pp. 395–407, 2018.

[25] VDI-3405 page 3, "VDI-Richtlinie: Additive manufacturing processes, rapid manufacturing: Design rules for part production using laser sintering and laser beam melting," 2017.

[26] F. Calignano, "Design optimization of supports for overhanging structures in aluminum and titanium alloys by selective laser melting," *Materials & Design*, vol. 64, pp. 203–213, 2014.

[27] M. Cloots, L. Zumofen, A. B. Spierings, A. Kirchheim, and K. Wegener, "Approaches to minimize overhang angles of SLM parts," *Rapid Prototyping Journal*, vol. 23, no. 2, pp. 362–369, 2017.

[28] T. Reiher „Intelligente Optimierung von Produktgeometrien für die additive Fertigung" Shaker Verlag, Dissertation, ISBN 978-3-8440-6728-6